Dynamic Modelling and Simulation of a Vectored Thrust Quad-Rotor

Benjamin Faul
School of Mechanical and
Manufacturing Engineering
University of New South Wales
Sydney, NSW 2052
Email: benjaminfaul@bigpond.com

Jay Katupitiya
School of Mechanical and
Manufacturing Engineering
University of New South Wales
Sydney, NSW 2052
Email: j.katupitiya@unsw.edu.au

***Abstract*—Current quad-rotor Unmanned Aerial Vehicles (UAVs) require changes in roll and pitch in order to move in the horizontal plane. This poses complications when the UAV is being used in applications that require steady visual imaging, such as surveillance, targeting and searching. The concept of a Vectored Thrust Aerial Vehicle (VTAV) overcomes this disadvantage of conventional quad-rotor UAVs. By changing the thrust direction of the propellers relative to its body, a quad-rotor VTAV can move in the horizontal plane without changing its attitude. Current modelling into VTAV systems has been very limited and restricted to many geometric assumptions. This paper presents the formulation of a quad-rotor VTAV model so that the concept may be tested more accurately. By deriving a mathematical model and performing open loop simulations in Matlab, the model is shown to overcome the limitations in motion that a conventional UAV faces. The result of this will lead to the realisation of various VTAV systems that can be implemented to create a stable aerial platform for image and video collection.**

I. Introduction

A. Background

Quad-rotors are the most popular aerial vehicle design for a number of reasons. Fixed pitch rotors mean that there are no complicated mechanical linkages, simplifying their construction and maintenance [1]. Vertical take off and landing as well as the high maneuverability and agility of quad-rotors gives them the ability to negotiate tight spaces with the potential for indoor use [2]. The ability to hover in a stationary position and fly at low velocities makes quad-rotors highly beneficial to many applications relating to image, video and data collection. Using four rotors instead of one gives quad-rotors a higher payload capacity than other UAV types, making them more useful for carrying sensor equipment [3] [4] [5]. More rotors also means the diameter of each rotor can be smaller, reducing the overall size of the system. Reducing rotor diameter also reduces the kinetic energy of the system: lower kinetic energy results in less damage to rotors and other objects in the case of a collision. More motors presents a disadvantage in the form of higher energy consumption, however this downfall is outweighed by the advantages described above. These advantages are the reason quad-rotors are considered the best aerial platforms for both experimentation and field applications such as surveillance, targeting, disaster monitoring (fire, flood, earthquake), search and rescue as well as hazmat spill monitoring and mobile sensor networks [2] [1]. Most of the applications that apply to quad-rotors require the ability to steadily and accurately focus sensors on a target location or to smoothly scan areas with cameras and other sensing equipment.

The conventional and most popular design for quad-rotors consists of 4 motors mounted on a cross shaped frame, with the motors at each corner of the frame. The motors are configured in pairs, with one pair rotating clockwise and the other pair rotating anticlockwise. The use of counter rotating motors helps eliminate the effects of aerodynamic torque and gyroscopic effects [1]. To control the motion of a quad-rotor, the individual motor speeds for each rotor are varied. By increasing or decreasing the motor speeds together, the quad-rotor moves in a vertical direction. By varying the difference between the forward and rear motors, the pitch of the quad-rotor is controlled resulting in forward and backward flight. Similarly by varying the left and right motors, roll is controlled resulting in left and right motion. Yaw is controlled by varying the difference in motor speeds between the counter rotating pairs. This produces an unbalanced torque about the vertical axis, producing a change in yaw or heading.

The major disadvantage of conventional quad-rotor UAVs is that the system is an underactuated system. This means that it is not possible to independently control each of the 6 degrees of freedom. A quad-rotor UAV cannot move left, right, forward or backwards without also experiencing a change in roll or pitch. This is related to the fact that there are 6 degrees of freedom but only 4 independent control inputs in the way of the rotor speeds. To overcome the problem of underactuation, the concept of a Vectored Thrust Aerial Vehicle (VTAV) has evolved. This increases the number of control inputs from 4 to 8 and eliminates the dependencies between pitch and forward/backward motion and roll and left/right motion.

The use of vectored thrust in small scale UAVs has only recently been explored and only implemented in a small number of cases for experimentation. Research into VTAVs

for developmental and commercial applications focuses on rotor aircraft such as quad-rotors. In 2007, Romero et al. designed and modelled a quad-rotor UAV with an additional 4 motors mounted perpendicular to the main rotors [6]. These additional rotors were for the purpose of achieving motion in the horizontal plane without any changes in pitch or roll of the aircraft. Their results showed a valid system with reasonable controllability and applicability. However this system suffers from a number of downfalls, including increased power consumption, aircraft size and motor torque imbalances.

Cetinsoy inproved this in 2012 and 2013 with his VTAV quad-rotor design. The design presented a quad-rotor with the addition of 4 control surfaces, one on each arm [7] [8]. These control surfaces rotated along the axis of the quad-rotor's arm and directed the airflow out of the rotors based on the angle of tilt. The downfall of this design is the size of the wings which greatly increases the aerodynamic drag and hence power consumption of the system.

Building on this design, there are a number of papers that implement a VTAV quad-rotor by tilting the main motors directly. By tilting each of the motors about the axis of the arm connecting them to the body of the quad, an overactuated system is achieved [2] [9]. This design makes the dynamic model of the system more complicated and significantly increases the difficulty of controller design. However, these difficulties are outweighted by achieving an over-actuated system that can potentially follow any arbitrary trajectory at fixed attitude configurations. The addition of 4 servos controls the angle of tilt for the 4 motors. Servo motors require very little power to actuate and can achieve very high size to torque ratio. This configuration also presents the simplest mechanism for tilting the motors whilst still achieving full independent control of the system's six degrees of freedom.

B. Layout

The organisation of this paper is as follows: Section 2 presents the derivation of the generalised VTAV system dynamic model by use of Newtonian mechanics. Section 3 presents the results from the simulation of various test cases and provides a discussion of these results. Section 4 concludes the paper, summing up the results and providing suggestions for future work.

II. Dynamic Modelling

A. Definition of Coordinate Frames

To calculate the forces acting on the quad-rotor during flight, two main coordinate systems are first defined. The coordinate frame B is fixed to the body of the quad-rotor with the origin fixed to the centre of mass. The x-axis points in the forward direction, the z-axis points straight down from body of the quad-rotor and the y-axis is in the direction that completes the right hand system. A second coordinate frame W is fixed in space. This coordinate frame represents the quad-rotors position and orientation in 3D space as shown in Fig. 1. Again the x-axis is in the forward direction, the z-axis points straight down and the y-axis completes the right hand system.

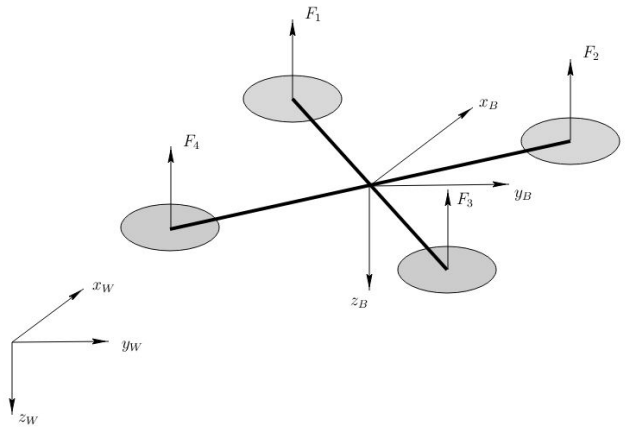

Fig. 1. VTAV coordinate frames in the world

To complete the system, four additional coordinate frames are attached to each motor assembly of the quad-rotor. These coordinate frames are located at the point where the quad-rotors arm axis intersects the axis of rotation of the motor. The x-axis points in the most forward direction, perpendicular to the arm axis. The z-axis points directly down and the y-axis is in the direction that completes the right hand coordinate system. A positive thrust angle θ_i causes the ith motor assembly coordinate frame to rotate positively about the y-axis. These motor assembly coordinate frames are denoted T_i where i is the motor assembly number as shown in Fig. 2. It is noted that in this diagram, the z axis is directed into the page. This figure also shows the direction of rotation for the rotors. The arm angles for each arm of the VTAV are also shown in the diagram and represented as θ_{Ai}, again where i is the number of the thruster assembly. The thruster assemblies are numbered from one to four with one being the front left motor, then preceding clockwise around the VTAV.

B. Forces in the Motor Assembly Frame

For each thruster group there is a thrust force generated by the spinning rotors. This rotation also causes a moment about the axis of rotation of the rotor. This moment depends on the direction of rotation. During vectoring, the rotation of the motor assembly about the axis of the quad-rotor arm creates a gyroscopic moment about the x-axis. These three forces and moments are shown graphically in Fig. 3.

The thrust force generated by each motor is defined in Eq. 1, where K_F is a constant defined by the geometry of the

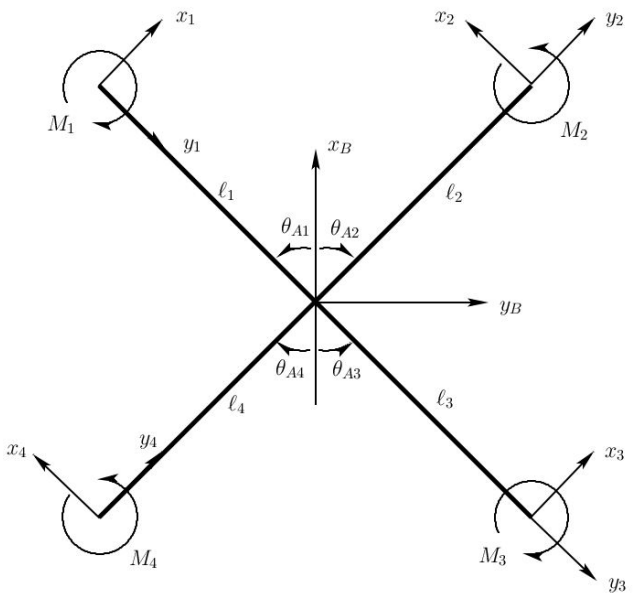

Fig. 2. VTAV coordinate frames

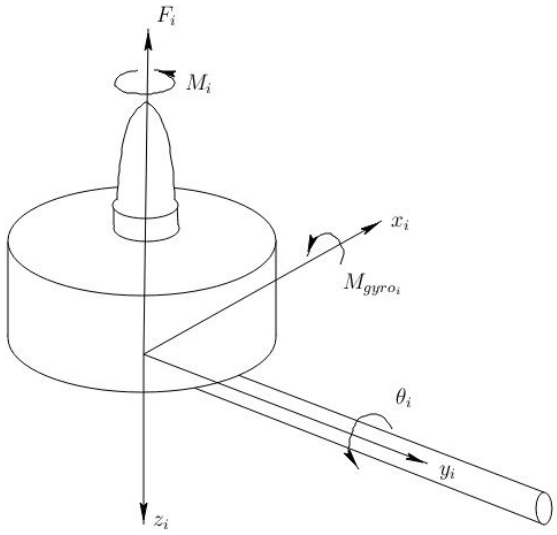

Fig. 3. Motor assembly free body diagram

rotor blades [1]. The motor speed is denoted ω_i where i is the number of the motor.

$$F_{T_i} = K_F \omega_i^2 \tag{1}$$

The torque generated from the propeller rotation is given in terms of the motor speed by Eq. 2. Here K_M is the motor torque constant [2].

$$M_{T_i} = K_M \omega_i^2 \tag{2}$$

The thrust force for each motor expressed in the corresponding motor frame is represented as follows. Since the thrust generated is in the upward direction, it acts in the negative z direction.

$$\boldsymbol{F_{T_i}} = \begin{bmatrix} 0 \\ 0 \\ -F_{T_i} \end{bmatrix} \tag{3}$$

Similarly the moment due to the motor torque is given by the following vector. It is noted here that the direction of the moment depends on the direction the motor is spinning. For motors 1 and 3 that are rotating clockwise, the z component of the moment is positive. For motors 2 and 4 it is negative.

$$\boldsymbol{M_{T_i}} = \begin{bmatrix} 0 \\ 0 \\ (-1)^{i+1} M_{T_i} \end{bmatrix} \tag{4}$$

The action of tilting the motor whilst the rotor is spinning causes a gyroscopic moment to be generated. This gyroscopic moment depends on the moment of inertia of the motor assembly, the rotor speed and the rate of thrust angle change, denotes as $\dot{\theta}_i$ [10]. The gyroscopic moment for each motor assembly is given in Eq. 3.5.

$$\boldsymbol{M_{gryo_i}} = \begin{bmatrix} I_{rot} \dot{\theta}_i \omega_i \\ 0 \\ 0 \end{bmatrix} \tag{5}$$

To translate these forces and moments from the motor assembly coordinate frame to the body coordinate frame, four individual transformation matrices are formed. These transformation matrices consist of a rotation only. This rotation simply expresses the thruster frame forces and moments with respect to the body frame, and does not translate them to the VTAV's centre of gravity. The translation of the thrust forces is detailed later. Each of the rotational matrices can be combined into one matrix since the rotational transform from each motor assembly group is by the variable arm angle. Each frame is rotated by the thrust angle θ_i and the arm angle θ_{Ai}. The only difference is the direction of some rotations. This is taken into account by the addition of the terms $(-1)^i$ and $(-1)^{i+1}$, with i being the motor assembly number. The combined rotational matrix is defined as follows. Note that s and c represent $\sin$ and $\cos$ respectively.

$${}^{\boldsymbol{B}}\boldsymbol{R_{Ti}} = \begin{pmatrix} s\theta_{Ai} c\theta_i & (-1)^i c\theta_{Ai} & s\theta_{Ai} s\theta_i \\ (-1)^{i+1} c\theta_{Ai} c\theta_i & s\theta_{Ai} & (-1)^{i+1} c\theta_{Ai} s\theta_i \\ -s\theta_i & 0 & c\theta_i \end{pmatrix} \tag{6}$$

In addition to this rotation matrix, a translation is required to complete the transformation from the thruster coordinate frame to the body coordinate frame [11]. This translation represents each of the thruster coordinate frame forces and moments as a force or moment about the VTAV's centre of gravity. By representing all forces and moments of the system about a single point, the system can then be modelled as a single point in space. The moments due to rotor spin and gyroscopic effects can be expressed in the body frame then translated freely to the VTAV's centre of gravity. For the thrust forces however, the translation from

the thruster frame to the VTAV's centre of gravity causes a moment to be generated. This translation is given as a vector in terms of the arm lengths and arm angles with respect to the quad-rotor's center of gravity. Note in the translation that the difference in the z-axis is assumed to be zero, that is the thruster coordinate frames are in the same horizontal plane as the body frame. The translation is given as:

$$^{\boldsymbol{B}}\boldsymbol{P}_{\boldsymbol{T_i}} = \begin{pmatrix} \eta_y \ell_i \cos\theta_{Ai} \\ \eta_x \ell_i \sin\theta_{Ai} \\ 0 \end{pmatrix} \tag{7}$$

In this equation η_x and η_y are constants that define the direction of the vector from each thruster coordinate frame to the body frame. The values for these constants are shown in the following table, where the thruster group is numbered according to the previous definition.

Thruster number	1	2	3	4
η_x	-1	-1	+1	+1
η_y	+1	-1	-1	+1

Fig. 4. Direction constants for thruster to body coordinate frame translations

C. Forces in the Body Coordinate Frame

Using the rotational matrix $^{B}R_{Ti}$ we can express each of the thrust forces in the body frame as:

$$\boldsymbol{F}_{\boldsymbol{B_i}} = {}^{\boldsymbol{B}}\boldsymbol{R}_{\boldsymbol{T_i}}\boldsymbol{F}_{\boldsymbol{T_i}} \tag{8}$$

The drag forces that act against the body during flight are experienced due to air friction and aerodynamic drag. The total drag on the system can be expressed as a single term based on the velocity the VTAV is moving in a direction. Therefore the combined effects of drag on the system are given by the following equation. This drag force acts in the direction opposite to the direction of thrust.

$$\boldsymbol{F_D} = \begin{pmatrix} C_x\dot{x} \\ C_y\dot{y} \\ C_z\dot{z} \end{pmatrix} \tag{9}$$

Here the terms C_x, C_y and C_z are the drag constants in the specified direction. Drag also occurs in rotational motion. The drag moments about each axis are similarly represented as the angular velocity about each axis multiplied by a drag constant. These drag moments are expressed as:

$$\boldsymbol{M_D} = \begin{pmatrix} C_\phi\dot{\phi} \\ C_\theta\dot{\theta} \\ C_\psi\dot{\psi} \end{pmatrix} \tag{10}$$

The moment generated due to the translation of the thrust forces from the origin of the thruster coordinate frames to the centre of gravity of the VTAV is expressed as in Eq. 11 where $\times$ represents the vector cross product.

$$\boldsymbol{M}_{\boldsymbol{B_{trans.}}} = {}^{\boldsymbol{B}}\boldsymbol{P}_{\boldsymbol{T_i}} \times \boldsymbol{F}_{\boldsymbol{B_i}} \tag{11}$$

The moment generated by the rotating propeller of each motor and the gyroscopic moments to the thrust vectoring are similarly transformed to the body frame using the rotational matrix $^{\boldsymbol{B}}\boldsymbol{R_{Ti}}$. Recall that these moments can then be regarded as acting about the centre of gravity of the VTAV.

$$\boldsymbol{M}_{\boldsymbol{B_i}} = {}^{\boldsymbol{B}}\boldsymbol{R}_{\boldsymbol{T_i}}\boldsymbol{M}_{\boldsymbol{T_i}} \tag{12}$$

$$\boldsymbol{M}_{\boldsymbol{B_{gyro_i}}} = {}^{\boldsymbol{B}}\boldsymbol{R}_{\boldsymbol{T_i}}\boldsymbol{M}_{\boldsymbol{gyro_i}} \tag{13}$$

The complete quad-rotor system is also subject to gyroscopic moments about each of the axes in the body frame. These moments are generated from each of the spinning rotors and the rotation of the body in terms of pitch and roll. Hence there will be four gyroscopic moments applied to the body frame. Change in yaw does not produce a gyroscopic moment on the system since this change is a rotation about the same axis as the propeller rotation [12]. These moments are calculated by the following equation.

$$\boldsymbol{M_{gyro_B}} = I_{rot}\omega_i \begin{pmatrix} \dot{\theta} \\ \dot{\phi} \\ 0 \end{pmatrix} \tag{14}$$

When vectoring each motor group, the servo motor produces a torque that is experienced by the body of the quad-rotor. Hence this torque is expressed in the body frame. Since the vectoring occurs about the axis of the quad-rotor arm, these moments are in the direction relative to the arm angles. The total effect of the servo torques is given in Eq. 15. This assumes that the vectoring mechanism is designed such that the servo torque is applied about the arm axis.

$$\boldsymbol{M_S} = \begin{pmatrix} M_{S1}s\theta_{A1} + M_{S2}s\theta_{A2} - M_{S3}s\theta_{A3} - M_{S4}s\theta_{A4} \\ -M_{S1}c\theta_{A1} + M_{S2}c\theta_{A2} + M_{S3}c\theta_{A3} - M_{S4}c\theta_{A4} \\ 0 \end{pmatrix} \tag{15}$$

The total moment of the VTAV can then be expressed in the body frame as the addition of each of the individual moments summed for each of the four motor assemblies.

$$\boldsymbol{M_{B_{total}}} = \boldsymbol{M_S} + \sum_{i=1}^{4} (\boldsymbol{M_{B_{transl}}} + \boldsymbol{M_{B_i}} + \boldsymbol{M_{gyro_i}}) - \boldsymbol{M_D} \tag{16}$$

The total force in the body frame is expressed as the sum of the thruster forces in the body coordinate frame for each thruster.

$$\boldsymbol{F_B} = \sum_{i=1}^{4} \left({}^{\boldsymbol{B}}\boldsymbol{R}_{\boldsymbol{T_i}}\boldsymbol{F}_{\boldsymbol{T_i}}\right) - \boldsymbol{F_D} \tag{17}$$

D. Forces in the World Inertial Frame

The only force that is applied to the quad-rotor in the world frame is the gravitational force. This is defined as below where

m is the total mass of the quad-rotor and g is the gravitational constant.

$$\boldsymbol{F_G} = \begin{pmatrix} 0 \\ 0 \\ mg \end{pmatrix} \tag{18}$$

To transform all of the forces and moments in the body coordinate frame to the world coordinate frame, the standard rotational matrix for the Euler angles pitch, roll and yaw is given by the following matrix [2]. The angles for pitch, roll and yaw are represented as θ, ϕ and ψ respectively. Note in the equation that cos and sin are expressed as c and s respectively.

$$^{W}R_B = \begin{pmatrix} c\psi c\theta & c\psi s\theta s\phi - s\psi c\phi & c\psi s\theta c\phi + s\psi s\phi \\ s\psi c\theta & s\psi s\theta s\phi + c\psi c\phi & s\psi s\theta c\phi - c\psi s\phi \\ -s\theta & c\theta s\phi & c\theta c\phi \end{pmatrix} \tag{19}$$

E. Assumptions

The quad-rotor experiences drag forces due to the spinning rotors and air friction when moving. However, it is assumed that the system will not be flow above a speed of 5m/s. In this case the combined drag forces have an insignificant effect on the system dynamics and can be ignored [13]. The viscous damping effects on the vectoring of the motor assemblies is also ignored. This damping constant could be estimated but would have an insignificant effect on the system dynamics since the small range of vectoring angles can be achieved very quickly using servo motors for actuation.

III. Simulation and Results

This chapter presents the results from the open loop simulation of the VTAV quad-rotor system. The results are explained and analysed to validate the system model. To demonstrate the validity of the VTAV model, a number of test cases were trialled using the simulation. Each of the following sections corresponds to a particular test case. The results from the simulation were plotted and will be shown in each section. Since the aim of this paper is to formulate and validate the dynamic model only, there is no control methods implemented in the simulation. Due to this, accumulating errors are observed. These errors will be discussed further in each case. By inverting the z axis plots, movement in the positive z direction represents actual upward movement.

The following simulations are all performed using the conventional 'X' configuration, as this configuration has been shown to perform with greater stability than other common configurations [14]. This is achieved by setting all the arm angles to $45°$.

A. Vertical Flight

This first test case involves the VTAV being flown directly up for a period time then flown back down to ground level. The purpose of this case is to demonstrate that the simple manoeuver of gaining then decreasing altitude does not have any effect on motion in the horizontal plane and no effect on pitch, roll and yaw angles. From the plots resulting from the simulation, it is observed that motion in the x and y directions is kept constant at zero. This is the desired result. The plot in Fig. 5 shows the x, y and z coordinates of the system during the test and the pitch, roll and yaw angles.

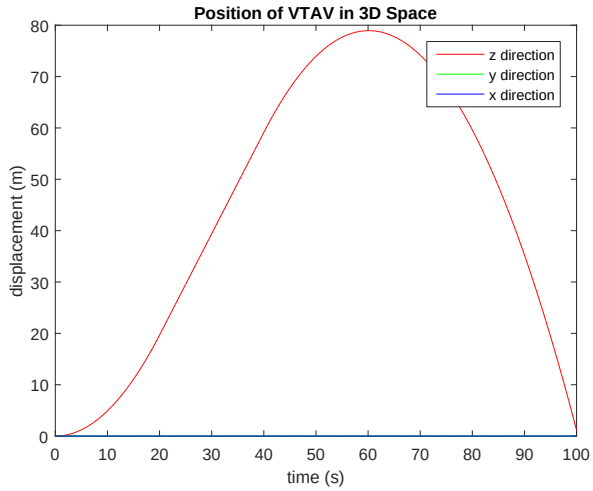

Fig. 5. x, y, z coordinates of VTAV for vertical flight

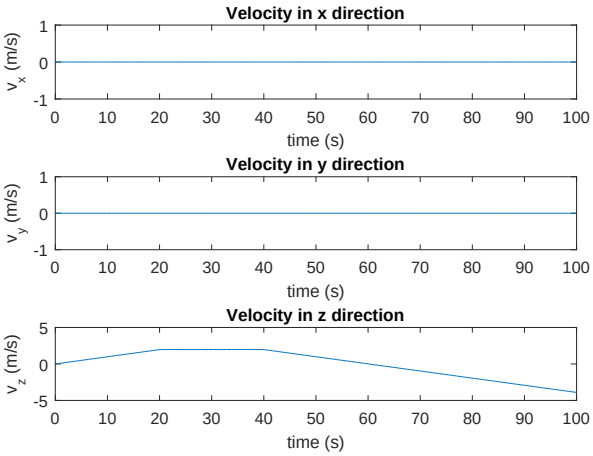

Fig. 6. Velocity in x, y, z direction for vertical flight

The velocity in each axis is also shown in Fig. 6. Throughout this simulation the pitch, roll and yaw angles as well as the thruster angles are all constant at zero.

B. Horizontal Flight

In this test case, the VTAV is initially hovering at a height of 300m. Then the motors are simultaneously pitched forward, then back to cause a forward trajectory. Figure 7 shows the result of this from the simulation. Note that as the rotors are vectored the forward displacement is increased. This causes a loss in altitude as expected as the motor speeds are not varied to compensate for the loss in vertical thrust.

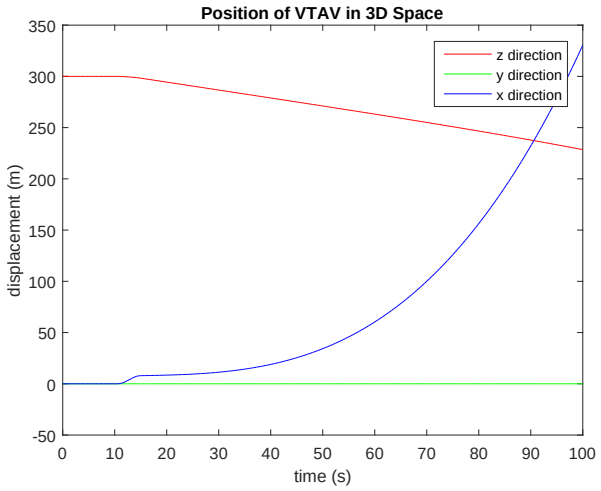

Fig. 7. Demonstration of motion in forward direction

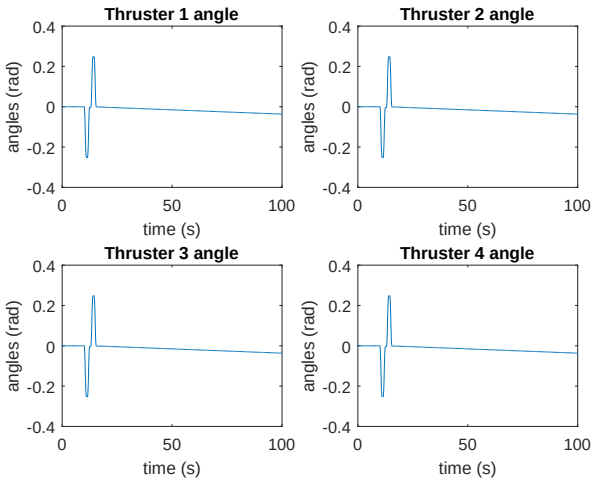

Fig. 8. Thruster angles showing effect of accumulated error

As expected, motion in the y direction is constant at zero. By showing this it can be concluded that the system is capable of independent control of position in the x coordinate. The system was also simulated to move in the y direction. The results above also pertain to motion in the y direction, due to the symetry of the VTAV system.

Since the simulation is open loop and therefore uncontrolled, it can be noted that when the input moments that create the vectoring of the motors is zero, the velocity does not steady at zero. This is due to the non-uniform time steps used in the integration process [15]. As the thrust angles are brought back to zero, the small accumulation of error causes a non-zero angular velocity for the thruster angles. This error causes the thrusters to be continuously rotating as shown in Fig. 8. It is observed that the x coordinate increases in an exponential way. However, in real life the inclusion of control systems and physical limitations on the thruster rotation would rectify this situation. Although this error causes the simulation to be very inaccurate at calculating position, the overall motion is in the desired direction. It is not possible to accurately measure distances traveled and velocities without control methods. Control is not required to validate the model since it is enough to show that the system responds with motion in the desired direction without variation in pose.

C. Yaw Control

The yaw angle of the VTAV system can be controlled using vectoring. By vectoring all the thrusters so that the horizontal forces are in the same direction around the perimeter of the square they form, the VTAV will rotate in that direction. This is demonstrated in Fig. 9. It is noted that when the thrusters are vectored, the loss in vertical thrust causes a loss in altitude as expected. The other method of controlling yaw is to change the motor speeds of the motor pairs as

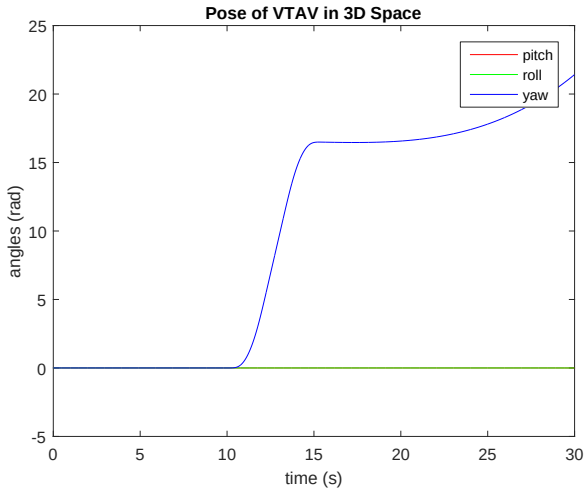

Fig. 9. Control of yaw using vectoring

performed by a conventional quad-rotor. All vectoring angles are kept at zero and only the motor speeds are changed. By doing this the drop in altitude is in the order of 10^{-6} and therefore negligible since the combined upward force can be kept constant.

The accuracy of the simulation is demonstrated in this test case by comparing two different methods of performing the same manoeuver. By changing yaw and therefore the heading of the system using vectoring, the error caused by the inaccuracy of applying thrust angle change is observed. On the other hand, controlling yaw using the conventional method of changing the speed of corresponding motor pairs, this thrust angle error is avoided. Therefore this result has significantly higher accuracy than vectoring. It is to be noted that this is due to a simulation error only and does not effect the validation of the dynamic model. With proper control methods, yaw control by vectoring would be possible with accuracy.

D. Independent Control of Pitch and Roll

Each of the three test cases above has demonstrated the independent control of four of the six degrees of freedom present in the VTAV system, namely x, y, z position and yaw control. This is already an advantage over conventional systems that do not have independent control of horizontal position. The independent control of pitch and roll is not explored in this work as it is not an ability required for many of the applications where VTAVs are useful. For any situation where a fixed pitch or roll angle is desired, the same result can be achieved by mounting sensing equipment at this angle and keeping the VTAV level.

IV. Conclusion

This paper has presented a comprehensive dynamic model of a vectored thrust aerial vehicle. By formulating this model, the concept of vectored thrust is validated for a quad-rotor UAV. The generality of the model allows for various configurations to be theorised and explored, while the completeness of the model creates a system that closer emulates a physical system. The simulations conducted in this work have shown that the 'X' configuration quad-rotor VTAV is a valid concept that achieves motion in the horizontal plane without changes in pitch and roll. The independent control of motion in the horizontal plane gives VTAV systems superior manoeuverability over conventional UAVs. Through the validation of the system, the VTAV concept can be applied to various applications that require a stable aerial platform. Applications in remote sensing that require this stability will benefit from VTAV systems as they will perform better in outdoor environments where external forces cannot be controlled or sufficiently counteracted.

The lack of control methods in this work means that the dynamic model cannot be simulated over complex paths and manoeuvers. Therefore the overall accuracy of positioning and flight dynamics cannot be tested. However it is shown that the VTAV model can perform movement in the horizontal plane independent of pitch and roll angles. This is the aim of the work presented in this paper and the validation of the model is achieved independent of the position and velocity accuracy. The implementation of control methods is suggested as the next step in future work, as well as the physical implementation of a VTAV system.

References

[1] R. M. Hossain, G. D. Rideout, and N. D. Krouglicof, "Bond graph dynamic modelling and stabilization of a quad-rotor helicopter," in *Proceedings of the 2010 Spring Simulation Multiconference*, 2010, pp. 215–223.

[2] A. Nemati and M. Kumar, "Modelling and control of a single axis tilting quadcopter," in *American Control Conference*, Portland, Oregon, 2014, pp. 3077–3082.

[3] K. Themistocleous, "The use of uav platforms for remote sensing applications: A case study in cyprus," in *International Conference on Remote Sensing and Geoinformation of the Environment*, 2014, pp. 92 290S–92 290S–9.

[4] S. Amici, M. Turci, F. Giulietti, S. Giammanco, M. F. Buongiorno, A. L. Spina, and L. Spampinato, "Volcanic environments monitoring by drones mud volcano case study," in *International Archives of Photogrammetry, Remote Sensing and Spatial Information Systems*, 2013, pp. 5–10.

[5] J. Everaerts *et al.*, "The use of unmanned aerial vehicles (uavs) for remote sensing and mapping," *The International Archives of the Photogrammetry, Remote Sensing and Spatial Information Sciences*, vol. 37, pp. 1187–1192, 2008.

[6] H. Romero, S. Salazar, A. Sanchez, and R. Lozano, "A new uav configuration having eight rotors: Dynamical model and real-time control," in *IEEE Conterence on Decision and Control*, 2007, pp. 6418–6423.

[7] E. Cetinsoy, "Design and simulation of a holonomic quadrotor uav with sub-rotor control surfaces," in *International Conference on Robotics and Biomimetics*, 2012, pp. 1164–1169.

[8] E. Cetinsoy, "Design and flight tests of a holonomic quadrotor uav with sub-rotor control surfaces," in *International Conference on Mechatronics and Automation*, 2013, pp. 1197–1202.

[9] M. Ryll, H. H. Bulthoff, and P. R. Giordano, "Modelling and control of a quadrotor uav with tilting propellers," in *IEEE International Conference on Robotics and Automation*, Saint Paul, Minnesota, 2012, pp. 4606–4613.

[10] W. Yuan, "Dynamic modelling and flight control methodologies for vertical take-off and landing unmanned aerial vehicles," Ph.D. dissertation, University of New South Wales School of Mechanical and Manufacturing Engineering, 2013.

[11] P. Corke, *Robotics, Vision and Control: Fundamental Algorithms in Matlab*, 1st ed. Springer-Verlag Berlin, 2013.

[12] R. C. Hibbler, *Engineering Mechanics: Dynamics*, 12th ed. Jurong, Singapore: Pearson Education Inc., 2010.

[13] W. Yuan and J. Katupitiya, "Dynamic modelling and control of a vectored thrust aerial vehicle," in *IEEE International Conference on Advanced Intelligent Mechatronics*, 2013, pp. 1361–1366.

[14] C. H. Kuo, C. M. Kuo, A. Leber, and C. Boller, "Vector thrust multi-rotor copter and its application for building inspection," in *International Micro Aerial Vehicle Conference and Flight Competition*, Toulouse, France, 2013, pp. 1–10.

[15] "Mathworks ode45 documentation," http://au.mathworks.com/help/matlab/ref/ode45/, accessed 27/5/2015.